

EFFECT OF Ni ON THE DIELECTRIC BEHAVIOR AND MICROWAVE ABSORPTION PERFORMANCE OF ZnO COMPOSITES

Samarjit Singh^{*}, Sushil Kumar Singh, Rahul Singh, Abhishek Kumar, Abhishek Nigam

Institute of Engineering & Technology Lucknow,

Sitapur Rd, Sector F, Jankipuram, Lucknow, Uttar Pradesh 226021, India

*e-mail: samarjitsingh05@gmail.com.

Abstract. In the present study, ZnO/Ni composites have been studied for its dielectric and microwave absorption behavior as a function of x (Ni/Zn-acetate ratio) viz. $x=0.08$, 0.12 , and 0.16 in the frequency range of 2-18 GHz. The hydrothermal method was successfully employed for the synthesis of single-phase Ni and ZnO particles. The phase confirmation was done using the X-ray diffraction technique and Maud refinement was successfully carried out using Maud software for the determination of crystallite size and the lattice parameters of pure Ni, pure ZnO, and $x=0.16$ sample. The inclusion of Ni in ZnO results in the improvement of complex permittivity values as compared to pure ZnO. However, there is not much significant enhancement in the complex permeability values. The microwave absorption characteristics are completely dependent on the dielectric properties of the composite materials. Ni incorporated ZnO composites show improvement in the microwave absorption characteristic as compared to pure ZnO. The improvement in microwave absorption behavior of the ZnO/Ni composite system may be ascribed to various mechanisms viz. dipole polarization, interfacial polarization, conduction loss, and impedance matching which synergistically acts to enhance the microwave absorption. A minimum reflection loss of -12.86 dB corresponding to > 90% absorption of incident microwave energy was observed for $x=0.16$ sample at a frequency of 17.47 GHz corresponding to 3 mm absorber thickness as compared to pure ZnO having a minimum reflection loss of -1.5 dB at the same absorber thickness.

Keywords: microwave absorption, Ni, ZnO, reflection loss, dipole polarization, interfacial polarization

1. Introduction

The use of electronic equipment in every sphere of human civilization encompassing from a normal household item to defense-based electronic systems has become the face of modern human society. This mammoth rise in the use of electronic systems has given rise to electromagnetic interference pollution problems that not only disrupt the proper working of the electronic circuits but also pose serious effects to the biological systems causing cell damage [1]. This electromagnetic pollution problem also affects the defense-based electronic systems and deteriorates their signals [2-4]. In today's time-based warfare, it is of utmost importance for the defense sector to camouflage its warheads from being detected by the enemy's radar tracking systems. The urgent need to minimize the electromagnetic pollution problem and impart stealth features to the defense systems has motivated researchers around the globe to develop efficient, high absorption, broad bandwidth, and light-weight microwave

absorbers [5,6]. However, all these favorable attributes cannot be sufficed by a single conventional material. Thus, material systems of composite nature are being studied and developed in order to integrate all the favorable attributes for the development of high-performance microwave absorbers. ZnO has been extensively used as optical scintillation ceramic and bio-ceramics but in the current study, the microwave absorption performance of ZnO composites has been studied [7,8].

In the present work, the microwave absorption response of the synthesized ZnO/Ni composites has been studied as a function of Ni/Zn-acetate ratio. The variation of Ni/Zn-acetate ratio dictates the dielectric properties of the composites for obtaining better impedance matching and realizing improved microwave absorption response. The presence of the composite system activates the interfacial polarization, defects polarization, and impedance matching which work synergistically to improve the microwave absorption response of the ZnO/Ni composites.

2. Experimentation Methodology

All the precursors were commercially available and used without further purification. Firstly, Ni particles were synthesized using the hydrothermal synthesis technique. In this procedure, 3.0 g of $\text{NiCl}_2 \cdot 6\text{H}_2\text{O}$ was dissolved in 30 ml deionized water. Then 3.0 g CTAB was added to 6.0 ml hydrazine hydrate solution ($\text{N}_2\text{H}_4 \cdot \text{H}_2\text{O}$, 80 wt.%). The CTAB/hydrazine mixture was added to the $\text{NiCl}_2 \cdot 6\text{H}_2\text{O}$ solution and thereby vigorously stirred for 40 minutes. The entire mixture was put in 50 ml capacity hydrothermal autoclave at 160°C for 6 hours. The black precipitates obtained were filtered and washed alternately with ethanol and water several times and dried at 60°C overnight. In the second step, the required amount of the synthesized Ni particles were added to the Zn-acetate solution dissolved in ethanol. The pH of the solution was maintained at 9 using 0.5M NaOH solution. The pH maintained alkaline solution was then kept at 110°C in a 50 ml capacity hydrothermal autoclave for 24 hours to get the ZnO/Ni composite precipitates. The ZnO/Ni precipitates were filtered and alternately washed with ethanol and water several times and finally dried at 60°C overnight. Pure ZnO was synthesized using a similar process in the absence of Ni particles.

The synthesized samples were characterized for phase analysis by recording the diffracted beam intensities using X-ray diffractometer (Rigaku Smartlab). Morphological analysis of the synthesized powders was executed using Scanning electron microscopy (SEM) images. Vector Network Analyzer (Agilent N5222 PNA series) was employed to determine the complex dielectric values of prepared samples in 2-18 GHz frequency range at room temperature. Cylindrically shaped pellets made by mixing the powder and epoxy in 80:20 weight ratio having an outer diameter of 7 mm and inner diameter of 3 mm was used for the dielectric measurement.

3. Results and Discussion

Phase analysis. The Maud refined X-ray diffraction pattern of the as-prepared samples is shown in Fig. 1. The phase identification, lattice parameters, and crystallite size for pure Ni, pure ZnO, and ZnO/Ni ($x=0.16$) were determined using Maud analysis. The crystal structure for Ni (ICSD: 646092) has been identified to be cubic with $a=b=c=3.5251 \text{ \AA}$ as the lattice parameters. The crystal structure for ZnO (ICSD: 57478) has been identified to be hexagonal with $a=b=3.256 \text{ \AA}$ and $c=5.218 \text{ \AA}$ as the lattice parameters. Maud refinement shows the successful synthesis of single-phase Ni and single-phase ZnO as shown in Figs. 1 (a) and (b), respectively, with 108 nm and 39 nm crystallite size. Figure 1 (c) contains only ZnO and Ni phase and no other impurity phase is present indicating successful synthesis of ZnO/Ni composites. The crystallite size of Ni and ZnO phases in the ZnO/Ni composites were found

to be 105 nm and 42.98, respectively, which are slightly different from their pure phase because of the strain fields which are created during the synthesis of the composite system.

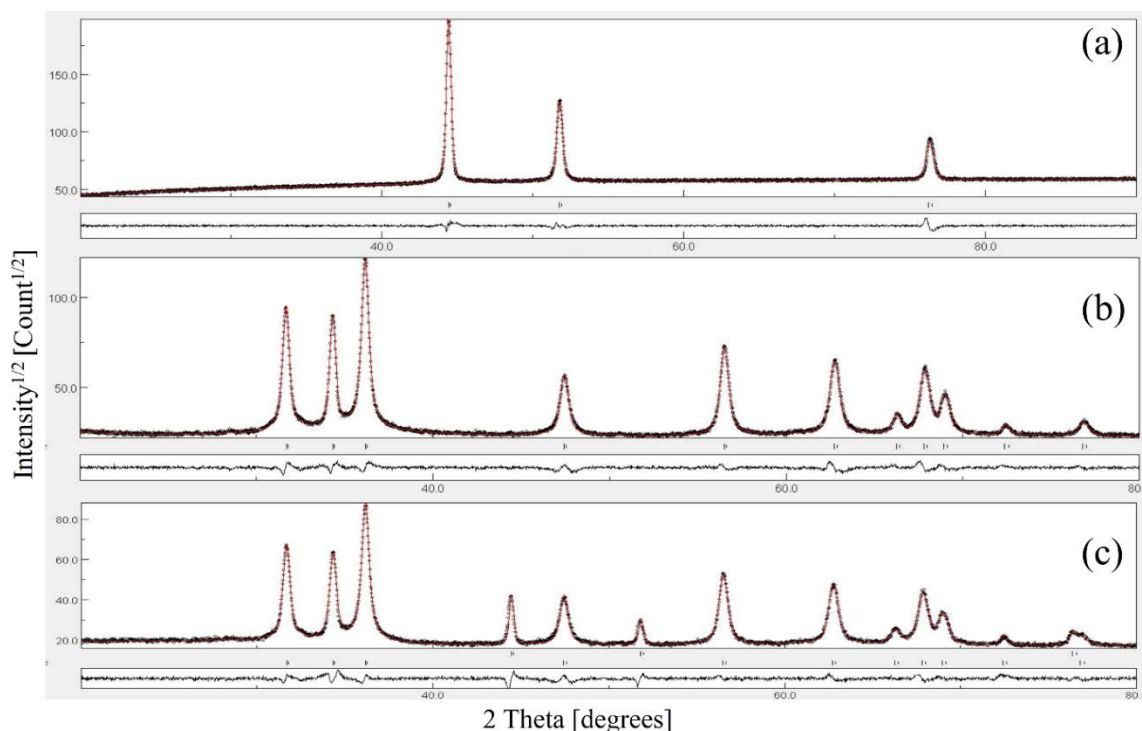


Fig. 1. Maud refined X-ray diffraction pattern for (a) Pure Ni and (b) Pure ZnO and (c) ZnO/Ni composites for $x = 0.16$

Morphological analysis. Figure 2 (a) depicts the spherical morphology of pure Ni particles with an average particle size of less than 1 μm . Figure 2 (b) clearly depicts the spherical morphology of pure ZnO. The ZnO/Ni ($x=0.16$) composite has more of a flaky nature and is much larger in size as compared to pure ZnO as shown in Fig. 2 (c). Pure ZnO nanoparticles' average size is about 50 nm while that of ZnO/Ni composite is around 2 μm . The larger size of ZnO/Ni composite is due to the presence of micron-sized Ni particles which act as sites for ZnO particles to grow. Apart from this, the Ni particles also tend to form a cluster of particles owing to their magnetic effect.

Dielectric study. Figures 3(a) and (b) represents the behavior of complex permittivity in the 2-18 GHz frequency range. It is evident from the figure that with the increase in Ni, the complex permittivity of the ZnO/Ni system also increases. This is attributed to the conductive nature of Ni particles. Another reason is the presence of intrinsic oxygen vacancy defects in ZnO structure. These oxygen vacancy defects act as polarization centers and induce dipole polarization. Therefore, as the amount of Ni in ZnO increases for $x = 0.12$ and 0.16 , causing an increase in the concentration of oxygen defects due to strain fields in the composite system which enhances the defect-induced dipole polarization effect. The complex permittivity for pure ZnO is low even though it is having the highest ZnO content. This is due to the fact that it contains a lesser number of defect sites as compared to the ZnO/Ni composite system. During the synthesis of ZnO in presence of Ni particles, ZnO will grow around Ni particles and these Ni particles might create some kind of strain fields dislodging the atoms from their usual site creating more defect sites in ZnO. Apart from dipole polarization, interfacial polarization also enhances the complex permittivity of the ZnO/Ni composite system. The presence of heterogeneous interfaces gives rise to interfacial polarization and hence the ZnO/Ni composite system has higher complex permittivity values compared to the pure ZnO. Higher ϵ'' signifies higher conductivity which is a direct consequence of the free electron

theory [9]. It has been found that electrical conductivity is significantly affected by the presence of oxygen vacancies in ZnO. The electrical conductivity increases with the increase in oxygen vacancies due to the reduction of the bandgap which translates into an increase in ϵ'' values [10]. The presence of conductive Ni particles also contributes to this effect. Therefore, for ZnO/Ni with $x = 0.16$ having a higher concentration of Ni particles as well as a higher concentration of oxygen vacancy defects translates into higher ϵ'' values as compared to the other samples. Figure 3(c) shows almost a constant value of μ' for the as-prepared samples. There is not much improvement in the values of μ' due to the presence of Ni particles owing to the dominance of dielectric behavior of ZnO. Figure 3(d) shows a decreasing trend in the behavior of μ'' with the increase in frequency. The curve for μ'' shows a steep change after 12 GHz owing to the natural and exchange resonance which might have come into play due to the small size and shape anisotropy effect. The complex permeability values are low but they play a very significant role in impedance matching; thereby affecting the microwave absorption response of the composite system.

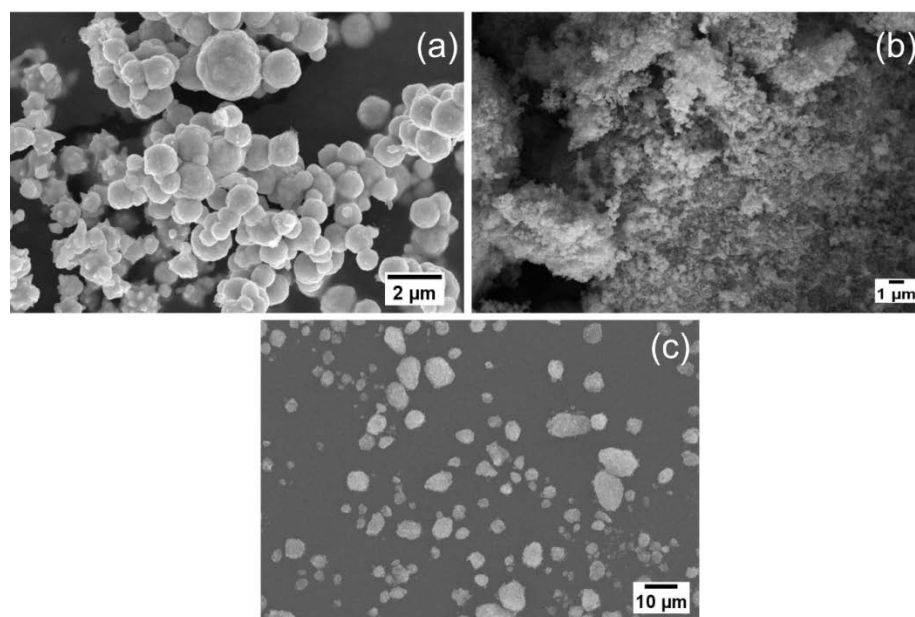


Fig. 2. SEM micrographs for (a) Pure Ni, (b) Pure ZnO and (c) ZnO/Ni composites for $x = 0.16$

Microwave absorption performance. The extent of microwave absorption is evaluated by the "Reflection loss" (RL) term which is used as an indicator to evaluate the microwave absorption capability of any material. Eqns. (1) & (2) are used to evaluate the microwave absorption capability [11, 12].

$$RL = 20 \log |(Z_{in} - Z_o)/(Z_{in} + Z_o)|, \quad (1)$$

$$Z_{in} = Z_o (\mu_r / \epsilon_r)^{1/2} \tanh \{j \cdot (2\pi ft/c) (\mu_r \cdot \epsilon_r)^{1/2}\}, \quad (2)$$

where each symbol represents its usual meaning. Figure 4 represents the RL behavior of the synthesized samples at 3 mm absorber thickness. The RL characteristics of the ZnO/Ni composite system have improved with the increase in the Ni content. This is ascribed to the defect-induced dipole and interfacial polarization mechanisms which contribute to the improvement of the microwave absorption behavior of ZnO/Ni composite system compared to the pristine ZnO system. The maximum microwave absorption response has been observed for $x=0.16$ sample. The minimum RL value for the corresponding sample was measured to be -12.86 dB at 17.47 GHz at 3 mm which is a significant increase as compared to pure ZnO having a minimum reflection loss of -1.5 dB at 3 mm absorber thickness.

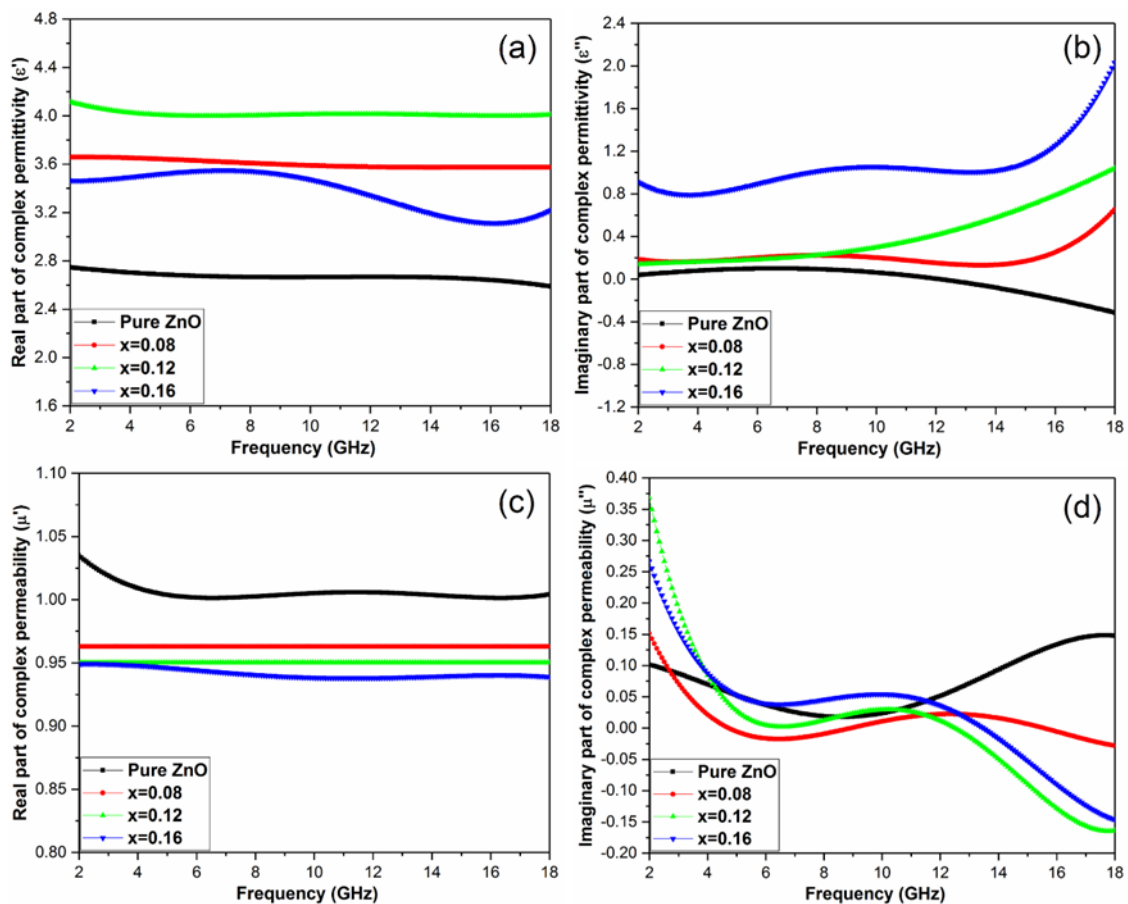


Fig. 3. (a) Real part of complex permittivity, (b) imaginary part of complex permittivity, (c) real part of complex permeability and (d) imaginary part of complex permeability with increasing frequency for ZnO/Ni composites

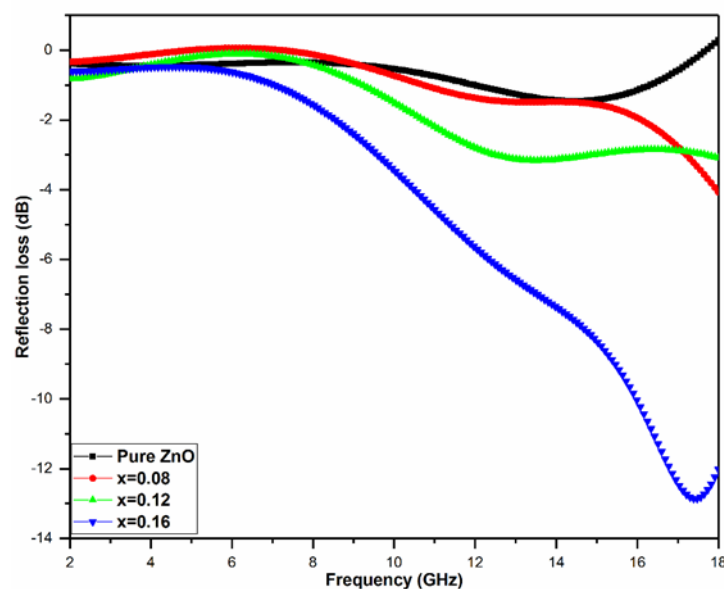


Fig. 4. Reflection loss curve as a function of frequency for ZnO/Ni composites

The impedance matching and attenuation constant for the synthesized samples have a strong correlation with the microwave absorption response. Equation 3 represents the

impedance matching factor $|Z_{in}/Z_0|$ that assesses the extent of matching between the complex permittivity and complex permeability values.

$$|Z_{in}/Z_0| = (\mu_r/\epsilon_r)^{1/2} \tanh \{j \cdot (2\pi ft/c) (\mu_r \cdot \epsilon_r)^{1/2}\}. \quad (3)$$

The samples which have $|Z_{in}/Z_0|$ values close to 1 have a strong tendency to exhibit better microwave absorption behavior. In a similar way, the attenuation constant (α) represents the ability to attenuate the incident microwaves [13]:

$$\alpha = \frac{\sqrt{2\pi f}}{c} \sqrt{(\mu''\epsilon'' - \mu'\epsilon') + \sqrt{(\mu''\epsilon'' - \mu'\epsilon')^2 + (\mu'\epsilon'' - \mu''\epsilon')^2}}, \quad (4)$$

where each symbol represents its respective meaning. Improvement in the microwave absorption properties is governed by the combined effect of impedance matching factor and attenuation constant. Figures 5 (a) and (b) show the impedance matching and attenuation behavior of the synthesized samples. Figure 5(a) shows that the impedance matching has increased significantly with the increase in Ni content in the ZnO/Ni composite system. Apart from this, Figure 5(b) shows the significant increase in the attenuation constant for $x=0.16$ sample. Better values of impedance matching and higher attenuation constant for $x=0.16$ sample has yielded better microwave absorption performance compared to $x=0.08$, 0.12 , and pure ZnO samples.

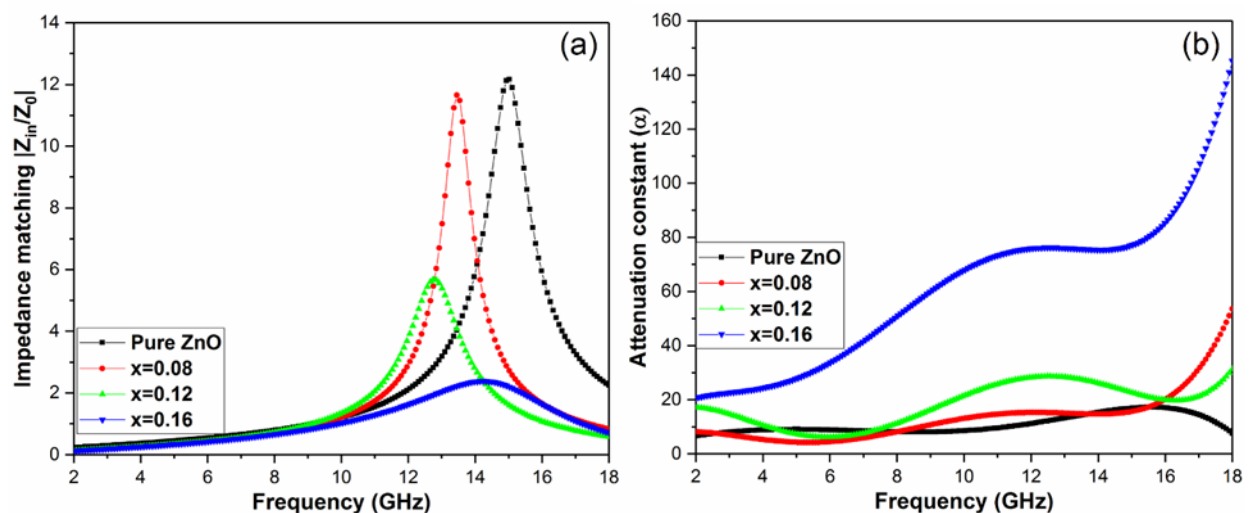


Fig. 5. (a) Impedance matching behavior at 3 mm absorber thickness and (b) attenuation constant curves as a function of frequency for ZnO/Ni composites

4. Conclusions

The present work manifests the successfully hydrothermal synthesis of single-phase Ni and ZnO particles. The dielectric and microwave absorption response of ZnO/Ni composites have improved with the minute addition of Ni particles in ZnO. Defect induced dipole polarization, interfacial polarization along impedance matching plays a very significant role in enhancing the microwave absorption performance of ZnO/Ni composites compared to pure ZnO. The minimum reflection loss of -12.86 dB at 17.47 GHz for an absorber thickness of 3 mm has been observed for $x=0.16$ sample reflecting a significant increase as compared to pure ZnO. Therefore, the amount of Ni in ZnO may be varied to obtain better microwave absorbers.

Acknowledgment. No external financial aid was provided for the present work. The authors would also like to thank Prof. Dharmendra Singh, IIT Roorkee for providing the VNA characterization facility.

References

- [1] Wang P, Cheng L, Zhang Y, Zhang L. Flexible SiC/Si₃N₄ composite nanofibers with in situ embedded graphite for highly efficient electromagnetic wave absorption. *Applied Materials and Interfaces*. 2017;9(34): 28844-28858.
- [2] Tian C, Du Y, Xu P, Qiang R, Wang Y, Ding D, Xue J, Ma J, Zhao H, Han X. Constructing uniform core-shell PPy@PANI composites with tunable shell thickness toward enhancement in microwave absorption. *ACS Applied Materials & Interfaces*. 2015;7(36): 20090-20099.
- [3] Feng Y, Qiu T. Enhancement of electromagnetic and microwave absorbing properties of gas atomized Fe-50 wt.% Ni alloy by shape modification. *Journal of Magnetism and Magnetic Materials*. 2012;324(16): 2528-2533.
- [4] Shen Z, Chen J, Li B, Li G, Zhang Z, Hou X. Recent progress in SiC nanowires as electromagnetic microwaves absorbing materials. *Journal of Alloys and Compounds*. 2020;815: 152388.
- [5] Wang P, Cheng L, Zhang L. One-dimensional carbon/SiC nanocomposites with tunable dielectric and broadband electromagnetic wave absorption properties. *Carbon*. 2017;125: 207-220.
- [6] Singh S, Kumar A. Selection of core shell material-based electromagnetic wave absorbers in 2-18 GHz using TOPSIS and VIKOR ranking methods. *Defence Science Journal*. 2019;69: 431-436.
- [7] Gorokhova EI, Eron'ko SB, Kul'kov AM, Oreshchenko EA, Simonova KL, Chernenko KA, Venevtsev ID, Rodnyi PA, Lott KP, Wiczorek H. Development and study of ZnO: In optical scintillation ceramic. *Journal of Optical Technology*. 2015;82(12): 837-842.
- [8] Rodnyi P, Venevtsev I, Gorokhova E, Eron'ko S, Boutachkov P, Saifulin M. Fast, Efficient, and Radiation Hard ZnO:In Ceramic Scintillator. In: *Proc. of the 2019 IEEE International Conference on Electrical Engineering and Photonics*. EExPolytech; 2019. p.197-200.
- [9] Singh S, Kumar A, Singh D. Enhanced microwave absorption performance of SWCNT/SiC composites. *Journal of Electronic Materials*. 2020;49(12): 7279-7291.
- [10] Bao X, Wang X, Zhou X, Shi G, Xu G, Yu J, Guan Y, Zhang Y, Li D, Choi C. Excellent microwave absorption of FeCO/ZnO composites with defects in ZnO for regulating the impedance matching. *Journal of Alloys and Compounds*. 2018;769: 512-520.
- [11] Singh S, Shukla S, Kumar A, Singh D. Influence of Zn dispersion in SiC on electromagnetic wave absorption characteristics. *Journal of Alloys and Compounds*. 2018;738: 448-460.
- [12] Singh S, Sinha A, Zunke RH, Kumar A, Singh D. Double layer microwave absorber based on Cu dispersed SiC composites. *Advanced Powder Technology*. 2018;29(9): 2019-2026.
- [13] Najim M, Smitha P, Agarwala V, Singh D. Design of light weight multi-layered coating of zinc oxide-iron-graphite nano-composites for ultra-wide bandwidth microwave absorption. *Journal of Materials Science: Materials in Electronics*. 2015;26: 7367-7377.